

Prediction of Binary and Ternary Diagrams Using the Statistical Associating Fluid Theory (SAFT) Equation of State

Felipe J. Blas and Lourdes F. Vega*

Departament d'Enginyeria Química, ETSEQ, Universitat Rovira i Virgili, Carretera de Salou s/n, 43006 Tarragona, Spain

A modified statistical associating fluid theory (SAFT) equation of state has been applied to predict the phase equilibria behavior of binary and ternary mixtures. In order to study multicomponent systems, the equation is first applied to pure fluids. The SAFT equation is written in the same spirit as that presented by Huang and Radosz [*Ind. Eng. Chem. Res.* 1990, 29, 2284–2294], but with two important differences: the reference term is a Lennard–Jones fluid, accounting explicitly for dispersive and repulsive forces, and the equation is extended to heteronuclear chains. The molecular parameters of pure substances are obtained by fitting to the saturated liquid density and by equating the chemical potentials in both phases. Three molecular parameters are needed to obtain the thermodynamic properties of pure substances, namely, the segment size, dispersive energy, and chain length. Two additional parameters are needed to describe the associating molecules, the association energy, and volume. They are obtained by fitting to experimental saturated liquid density and by equating the chemical potentials in both phases over a wide range of temperatures. The molecular parameters are found to scale with the molecular weight for the alkanes. The binary parameters of the mixtures, ξ_{12} and η_{12} in the generalized Lorentz–Berthelot combining rules, are fitted to experimental data for the molar fractions on the liquid and vapor sides at a given temperature, in such a way that they do not depend on the composition and/or temperature. These binary parameters are used to predict the behavior of the mixture at different thermodynamic conditions. Ternary mixtures are predicted from the previous parameters without any further adjustment. The agreement between prediction and experimental results is excellent in all cases.

Introduction

In recent years much effort has been devoted to the development of molecular-based equations of state (EOS). The advantage of these equations versus most traditional equations of state is that, in addition to providing a thermodynamic basis for deriving chemical potentials and fugacities (needed for phase equilibria calculations), they also allow for separating and quantifying the effects of molecular structure (chain length) and interactions (polarity, hydrogen bonds, etc.) on bulk properties and phase behavior. The fact that they have a molecular basis, that is, parameters with physical meaning and few in number, makes them reliable when making extrapolations or predictions at other thermodynamic conditions.

The statistical associating fluid theory (SAFT) is one of these approaches which has received great attention from the beginning. The equation is based on Wertheim's first-order thermodynamic perturbation theory for associating fluids (Wertheim, 1984a,b, 1986a–c, 1987), using hard spheres as the reference fluid. The original SAFT equation was independently developed from Wertheim's theory by Chapman (1990a,b), Chapman et al. (1988), Jackson et al. (1988), Joslin et al. (1987), and Wertheim (1987). The equation has been extended to Lennard–Jones (Chapman, 1990; Banaszak et al., 1994) and square-well systems (Banaszak et al., 1993) and has been extensively tested against computer

simulations (Johnson and Gubbins, 1992; Ghonasgi and Chapman, 1993a,b, 1994a; Walsh and Gubbins, 1993; Müller et al., 1994, 1995; Johnson et al., 1994; Banaszak et al., 1993, 1994) and experimental results (see, for example, Huang and Radosz, 1990, 1991; Fu and Sandler, 1995; Galindo et al., 1996, 1997). The SAFT equation has been modified by considering a reference fluid of dimers, instead of monomers (Chang and Sandler, 1994; Ghonasgi and Chapman, 1994b; Tavares et al., 1995), providing a better description of chain molecules. The SAFT approach has also been modified to deal with different attractive potentials, that is, chain molecules of hard-core segments with attractive potentials of variable range, the so-called SAFT-VR (Gil-Villegas et al., 1997).

In the SAFT equations of state of Huang and Radosz, and Fu and Sandler, the residual Helmholtz free energy for a pure component has four contributions: the hard-sphere, dispersion, chain, and association terms. The hard-sphere, chain, and association terms are derived from statistical thermodynamics and are identical in both cases. For the dispersion term Huang and Radosz used a double-power series in density and temperature fitted to the argon physical properties data by Chen and Kreglewski (1977). Fu and Sandler proposed what they called the simplified SAFT EOS by using the single attraction term of Lee et al. (1985) instead of the multiterm double-series dispersion term, resulting in a simpler equation of state. Galindo et al. (1996) give the contribution due to the dispersive attractive interactions at a mean field level in terms of the van der Waals one-fluid theory of mixing.

* Author to whom correspondence should be addressed.
E-mail: lvega@etseq.urv.es.

Recently, Economou and Tsonopoulos (1997) have used three different equations of state to obtain an accurate description of water/hydrocarbon phase equilibria. Results from these authors show that a traditional cubic equation of state, such as the Rendlich–Kwong–Joffe–Zudkevitch (RKJZ) (Zudkevitch and Joffe, 1970), gives better results than APACT (Ikonomou and Donohue, 1986; Economou and Donohue, 1992) and the original version of SAFT (Chapman et al., 1990; Huang and Radosz, 1990). As pointed out by the authors, a more realistic dispersion term in the SAFT equation, such as the Lennard–Jones, will probably improve the predictions for the hydrocarbon solubility in water.

Blas and Vega (1997) have proposed a modified version of SAFT (soft-SAFT), based on the extension of Wertheim's theory to Lennard–Jones chains by Johnson et al. (1994), where the residual Helmholtz free energy of the mixture is given by the addition of three contributions (instead of four): the dispersive and repulsive terms are taken into account by using a Lennard–Jones fluid as the reference fluid, while chain and association terms are the same as in the previous approaches. This version of SAFT is valid for heteronuclear chains, making it a general equation of state, applicable to spherical molecules, homonuclear and heteronuclear chain molecules, associating and nonassociating molecules, pure fluids, and mixtures.

The aim of the present work is to apply this SAFT EOS (Blas and Vega, 1997) to predict thermodynamic properties, as well as liquid–vapor equilibria, of binary and ternary mixtures of hydrocarbons. We first calculate the molecular parameters of the *n*-alkane series. To show that the same equation is applicable to other different fluids, the 1-alkene and 1-alkanol series are also studied. The molecular parameters of the pure compounds have been determined by fitting them to experimental data for vapor pressure and saturated liquid density and have been shown to depend linearly on molecular weight. Several binary mixtures of hydrocarbons have been studied at different conditions. We have calculated the behavior of some binary mixtures from the molecular parameters of the pure components, hence *predicting* the mixture behavior. In some cases binary parameters are needed. These parameters, ξ_{12} and η_{12} in the generalized Lorentz–Berthelot combining rules, are fitted to experimental data for the molar fractions on the liquid and vapor sides at a given temperature, in such a way that they do not depend on the composition and/or temperature. Ternary mixtures (methane–ethane–propane and ethane–butane–heptane) at different temperatures and pressures are predicted from the previous parameters without any further adjustment.

The paper is organized as follows: we first present the main features of the molecular model used, as well as the equation of state and the fitting procedures, followed by results and discussion. Conclusions are given in the last section.

Equation of State

Since the philosophy of the SAFT EOS and its technical issues have been treated in detail previously (see, for example, Galindo et al., 1996 and references therein) we will explain here just the model used for the different substances of interest in the present study and the most important features concerning our extension and the approximations made.

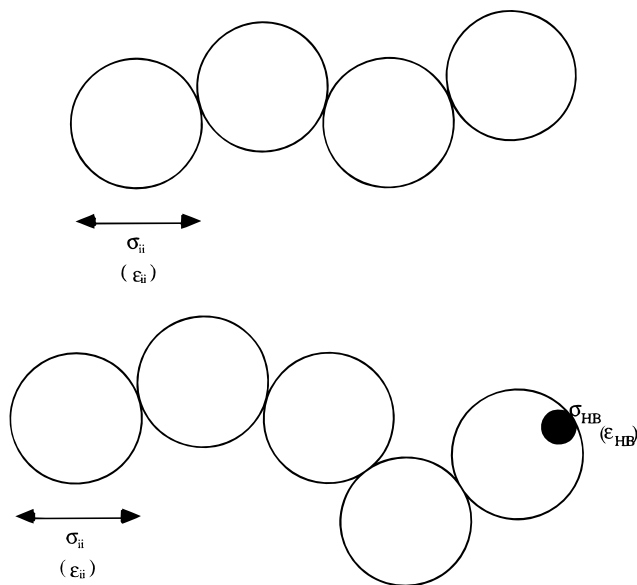


Figure 1. (a) Two-dimensional view of the homonuclear associating chain. The large circles represent the Lennard–Jones cores and the small circle is an associating site. (b) Two-dimensional view of a heteronuclear nonassociating Lennard–Jones chain with different segment sizes and dispersive energies.

n-Alkanes, 1-alkenes, and 1-alkanols are described as homonuclear chainlike molecules. This is an approximation since the actual molecules are heteronuclear due to the presence of different chemical groups, such as CH₃, CH₂, and/or CH, and it has been used previously (Huang and Radosz, 1990, 1991; Fu and Sandler, 1995; Galindo et al., 1996). When the number of carbon atoms increases, the amount of CH₂ groups *versus* CH₃ and/or CH increases largely, in such a way that most of the segments of the molecules are composed only by these chemical groups. In this situation, the chains are almost homonuclear, making the approximation better.

Molecules are represented as united atoms or sites: each site is assigned parameter values to represent a specific atom or group of atoms in the molecule of interest. The site–site interaction potentials are the microscopic molecular analogue of the group contribution engineering models. In contrast to macroscopic models, the molecular structure is well-defined at the microscopic level. These models attempt to strike a balance between simplicity, in order to make calculations possible, and enough complexity to quantitatively predict the behavior of interest. Care must be taken when using the molecular parameters given in this work for other applications: although the molecular parameters have physical meaning (segment diameter, dispersive energy per segment, and chain length), they are *effective* parameters. This is due to the fact that we use a Lennard–Jones potential, instead of an *ab-initio* potential.

Homonuclear chain molecules are modeled as *m* Lennard–Jones segments of equal diameter σ , and the same dispersive energy ϵ , bonded tangentially to form the chain, as shown in Figure 1a. Intermolecular and intramolecular dispersive energies are taken into account through the Lennard–Jones potential:

$$\phi = 4 \sum_i \sum_j \epsilon_{ij} \left[\left(\frac{\sigma_{ij}}{r} \right)^{12} - \left(\frac{\sigma_{ij}}{r} \right)^6 \right] \quad (1)$$

This model accounts for three important attributes of chain molecular architecture, that is, the bead connectivity, to represent topological constraints and internal flexibility, the excluded volume effects, and the attraction between different beads. Although the model is simple compared to more realistic models, it conserves the relevant features of the real system. Hence, we expect to give good results and to predict accurately the thermodynamic properties as well as the phase equilibria.

For associating molecules with specific interactions, such as 1-alkanols, additional parameters are needed. The hydrogen bond energy is accounted for with some embedded off-center square-well bonding sites (see Figure 1b). A two-sites model for 1-alkanols is used (Müller and Gubbins, 1995; Gupta and Johnston, 1994). Following Müller et al. (1994, 1995), the associating sites are modeled as square-well sites placed at a distance b from the center of the Lennard–Jones core. The depth of the energy well is ϵ^{HB} , and σ^{HB} is the diameter of the site:

$$\phi^{\text{HB}} = \begin{cases} -\epsilon^{\text{HB}} & \text{if } r_{\text{AB}} \leq \sigma^{\text{HB}} \\ 0 & \text{otherwise} \end{cases} \quad (2)$$

where r_{AB} is the square well–square well site–site distance. Two molecules are considered bonded when r_{AB} is smaller than σ^{HB} .

The equation of state is written in terms of the Helmholtz free energy. The residual Helmholtz free energy for an n -component mixture of associating chain molecules can be expressed as a sum of three terms: a reference term, A^{ref} , including the repulsive and the attractive energies, a chain term, A^{chain} , and a perturbation term, A^{assoc} , which explicitly takes into account the contribution due to the association,

$$\frac{A}{N_{\text{m}}k_{\text{B}}T} - \frac{A^{\text{ideal}}}{N_{\text{m}}k_{\text{B}}T} = \frac{A^{\text{ref}}}{N_{\text{m}}k_{\text{B}}T} + \frac{A^{\text{chain}}}{N_{\text{m}}k_{\text{B}}T} + \frac{A^{\text{assoc}}}{N_{\text{m}}k_{\text{B}}T} \quad (3)$$

where N_{m} is the number of chain molecules in the system, k_{B} the Boltzmann constant, and T the temperature. In this work, the reference term is taken from a Lennard–Jones fluid. Chain molecules are modeled as freely jointed Lennard–Jones spheres with a fixed bond distance equal to the diameter of spheres (see Figure 1a). For more details, see Blas and Vega (1997).

Ideal Term

The form of A^{ideal} in eq 3 for the case of a multicomponent system is

$$\frac{A^{\text{ideal}}}{N_{\text{m}}k_{\text{B}}T} = \sum_{i=1}^n (x_i \ln \rho_{\text{m}}^{(i)} \Lambda_i^3) - 1 \quad (4)$$

The sum is over all species i of the mixture, $x_i = N_{\text{m}}^{(i)}/N_{\text{m}}$ is the molar fraction, $\rho_{\text{m}}^{(i)} = N_{\text{m}}^{(i)}/V$ the molecular density, $N_{\text{m}}^{(i)}$ the number of molecules, Λ_i the thermal de Broglie wavelength, and V the volume of the system. ρ_{m} , the total number of chains divided by the volume, can be related to the total monomeric density by

$$\rho = \left(\sum_{i=1}^n m_i x_i \right) \rho_{\text{m}} = \sum_{i=1}^n m_i \rho^{(i)} \quad (5)$$

being $\rho^{(i)} = x_i \rho_{\text{m}}$ the monomeric density of species i and m_i its chain length.

Lennard–Jones Reference Term

The reference term accounts for the repulsive and attractive interactions of the segments forming the chains. A^{LJ} is the Helmholtz free energy of a mixture of spherical Lennard–Jones. In this work we choose the Lennard–Jones EOS proposed by Johnson et al. (1993), although any other choice would be equally appropriate (Bokis and Donohue, 1995). This equation is an extended Benedict–Webb–Rubin equation of state that was fitted to simulation data for pure Lennard–Jones fluids over a broad range of temperatures and densities.

Chain Term

The expression for the contribution of the formation of the chain takes a different form for homonuclear and heteronuclear chains. For the first case, the free energy contribution was independently derived by Wertheim (1987), Chapman et al. (1988), and Jackson et al. (1988) from the first-order perturbation theory for associating spherical molecules. Starting from a mixture of spherical molecules with the correct stoichiometry and the associating sites on the right positions to allow the bonding of different segments, the formation of the chain is obtained by setting the fraction of monomers equal to zero.

For a mixture of chains with bond length equal to σ_{ij} , the diameter of the Lennard–Jones in the species i , the final expression can be written as (Ghonasgi and Chapman, 1994a–c; Johnson et al., 1994):

$$\frac{A^{\text{chain}}}{N_{\text{m}}k_{\text{B}}T} = \sum_{i=1}^n x_i (1 - m_i) \ln y_{\text{R}}^{(i)}(\sigma_{ii}) \quad (6)$$

where m_i has been previously defined and $y_{\text{R}}^{(i)}(\sigma_{ii})$ is the contact value of the cavity correlation function for spherical segments of species i in the Lennard–Jones reference fluid. $y_{\text{R}}^{(i)}(\sigma_{ii})$ is given by $y_{\text{R}}^{(i)}(\sigma_{ii}) = g_{\text{R}}^{(i)}(\sigma_{ii}) \exp(\phi_{\text{LJ}}(\sigma_{ii})/k_{\text{B}}T)$, with $g_{\text{R}}^{(i)}(\sigma_{ii})$ the pair radial distribution function of the Lennard–Jones fluid.

The SAFT-EOS has recently been extended to describe heteronuclear chains (Archer and Jackson, 1991; Amos and Jackson, 1991; Banaszak et al., 1996; Blas and Vega, 1997). The free energy term due to the formation of chains may be derived using the same procedures and approximations as those used to obtain homonuclear chains (eq 6): starting with a mixture of Lennard–Jones spheres (with different segment size and/or dispersive energy) with appropriate associating sites and stoichiometry and taking the limit of complete bonding, the chain term may be expressed as

$$\frac{A^{\text{chain}}}{N_{\text{m}}k_{\text{B}}T} = - \sum_{i=1}^n x_i \sum_{j=1}^{m_i-1} \ln y_{\text{R}}(\sigma_{j,j+1}^{(i)}) \quad (7)$$

where x_i and m_i have been previously defined and $y_{\text{R}}(\sigma_{j,j+1}^{(i)})$ is the contact value of the cavity correlation function for spherical segments of species j and $j+1$ in the reference Lennard–Jones fluid. The superscript denotes the contribution to chain i . It may be expressed, as for homonuclear chains, in terms of the pair radial distribution function of the Lennard–Jones system.

In both cases, homonuclear and heteronuclear chains, a closed equation of state is obtained, replacing the pair distribution function of the reference fluid by the pair radial distribution function of free Lennard–Jones spheres evaluated at the temperature and density of the mixture. Accurate results of Johnson and Gubbins (1992) are used for the pair radial distribution function of the Lennard–Jones fluid.

Association Term

The Helmholtz free energy contribution due to association, valid for homonuclear and heteronuclear chains, is given by the first-order Wertheim's perturbation theory for associating fluids. The term is expressed by a sum over the contributions of all $n(\Gamma^{(i)})$ sites of each species i , weighted by the molar fraction

$$\frac{A^{\text{assoc}}}{N_m k_B T} = \sum_{i=1}^n x_i \left[\sum_{A \in \Gamma^{(i)}} \left(\ln X_A^{(i)} - \frac{X_A^{(i)}}{2} \right) + \frac{1}{2} n(\Gamma^{(i)}) \right] \quad (8)$$

where the sum runs over the species i and all the associating sites of molecules i . $X_A^{(i)}$, the fraction of nonbonded sites A of molecules i , may be written as a mass-action equation:

$$X_A^{(i)} = \frac{1}{1 + \sum_k x_k \rho_k \sum_{B \in \Gamma^{(k)}} X_B^{(k)} \Delta_{AB}^{(ik)}} \quad (9)$$

All the non-zero site–site interactions should be defined *a priori* in order to solve eq 9. $\Delta_{AB}^{(ik)}$ involves an unweighted integral over all the orientations and an integration over all separations of molecules 1 and 2, defined as

$$\Delta_{AB}^{(ik)} = \int g_{LJ}^{(ik)}(12) f_{AB}^{(ik)}(12) d(12) \quad (10)$$

with $g_{LJ}^{(ik)}(12)$ the pair distribution function of the reference fluid, $f_{AB}^{(ik)}(12) = \exp(\epsilon_{AB}^{\text{HB}}/k_B T) - 1$ is the Mayer function of the association potential, and $d(12)$ denotes an unweighted average over all orientations and an integration over all separations of molecules 1 and 2.

The integration of eq 10 is not straightforward, since the pair distribution function is not readily available. We have replaced the pair distribution function of the Lennard–Jones chain fluid by the pair distribution function of the Lennard–Jones segment fluid, evaluated at the same temperature and segment density. The choice of this approximation and its validity has been discussed previously (Müller et al., 1994). In order to accurately calculate the integral (10), the expression from Müller and Gubbins (1995) for a particular position of the association site inside the Lennard–Jones sphere has been used.

Extension to Mixtures

To extend the equation of state to mixtures, we need to consider how to do it with each contribution to the Helmholtz free energy. In the SAFT version we apply here, only the reference term needs to be extended to

mixtures. The chain and association terms depend explicitly on composition; thus, they are readily applicable to mixtures. The simplest and most common way to extend the Lennard–Jones equation of state to mixtures is by using the conformal solution theory (Hansen and McDonald, 1980). In this work we have used the van der Waals one-fluid theory (vdW-1f). A discussion on the appropriateness of this rule as well as some other mixing rules also applicable to these systems can be found elsewhere (Blas and Vega, 1997).

The Helmholtz free energy of the *mixture* of spherical Lennard–Jones may be described by the EOS of Johnson et al. (1993), using vdW-1f. In this theory, the residual Helmholtz free energy of a mixture is approximated by the residual Helmholtz free energy of a pure hypothetical fluid, with parameters σ_m and ϵ_m calculated from

$$\sigma_m^3 = \frac{\sum_{i=1}^n \sum_{j=1}^n m_i m_j x_i x_j \sigma_{ij}^3}{\sum_{i=1}^n \sum_{j=1}^n m_i m_j x_i x_j} \quad (11)$$

$$\epsilon_m \sigma_m^3 = \frac{\sum_{i=1}^n \sum_{j=1}^n m_i m_j x_i x_j \epsilon_{ij} \sigma_{ij}^3}{\sum_{i=1}^n \sum_{j=1}^n m_i m_j x_i x_j} \quad (12)$$

These expressions are the traditional mixing rules for a mixture of Lennard–Jones segments, expressed as a function of chain molar fractions, instead of segment molar fractions. We have used the relationship between both molar fractions, namely

$$X_i = \frac{m_i x_i}{\sum_{k=1}^n m_k x_k} \quad (13)$$

where X_i is the molar fraction of Lennard–Jones segments of species i .

To obtain the pair correlation function of a mixture of LJ spheres, the same mixing rules have been used. The van der Waals one-fluid equation for the pair radial distribution function of component i interacting with component j is

$$g_R^{(ij)}(r) = g_m(r^*, \rho_m^*, T_m^*) \quad (14)$$

where $g_m(r^*, \rho_m^*, T_m^*)$ is the radial distribution function for a *pure LJ fluid* with $r^* = r/\sigma_m$, $T_m^* = k_B T/\epsilon_m$, and $\rho_m^* = \rho \sigma_m^3$ (ρ is the total monomeric density of the mixture). σ_m and ϵ_m are given by eqs 11 and 12, respectively.

For the crossed interactions, the generalized Lorentz–Berthelot combining rules are used:

$$\sigma_{ij} = \eta_{ij} \frac{\sigma_{ii} + \sigma_{jj}}{2} \quad (15)$$

$$\epsilon_{ij} = \xi_{ij} \sqrt{\epsilon_{ii} \epsilon_{jj}} \quad (16)$$

The applicability of the van der Waals one-fluid theory (Hansen and McDonald, 1980) for binary and ternary

mixtures of Lennard–Jones spheres has proved to be excellent in previous studies (Harismiadis et al., 1991; Georgoulaki et al., 1994; Panagiotopoulos, 1987, 1992; Tsang et al., 1995). It has also been tested against molecular simulations for Lennard–Jones chains with different segment sizes and dispersive energies (Blas and Vega, 1997), showing excellent results even for highly asymmetric mixtures. The subscripts i and j refer to different segments belonging to the same chain or different chains.

Fitting Procedures

To calculate the molecular parameters of pure substances, σ , ϵ , and m , and ϵ^{HB} and k^{HB} , in the case of associating molecules, we have fitted to experimental data for vapor pressure and saturated liquid density over a wide range of temperatures, defining two functions, depending on the parameters to be found:

$$f_1(\sigma, \epsilon, m, \epsilon^{\text{HB}}, k^{\text{HB}}) = \sum_{i=1}^N \{\rho_i^{\text{exp}} - \rho_i^{\text{calc}}(p_i^{\text{exp}}, T_i^{\text{exp}})\}^2 \quad (17)$$

$$f_2(\sigma, \epsilon, m, \epsilon^{\text{HB}}, k^{\text{HB}}) = \sum_{i=1}^N \{\mu_{i,\text{liq}}^{\text{calc}}(p_i^{\text{exp}}, T_i^{\text{exp}}) - \mu_{i,\text{vap}}^{\text{calc}}(p_i^{\text{exp}}, T_i^{\text{exp}})\}^2 \quad (18)$$

where N is the number of experimental points used in the fitting, i is the label for every experiment used, T_i^{exp} , ρ_i^{exp} , and p_i^{exp} are the temperature, the saturated liquid density, and the vapor pressure corresponding to the experimental point i . ρ^{calc} is the saturated liquid density predicted by the EOS at the temperature T_i^{exp} . $\mu_{i,\text{liq}}^{\text{calc}}$ and $\mu_{i,\text{vap}}^{\text{calc}}$ are the chemical potentials of the liquid and vapor side, respectively, predicted by the EOS at the temperature T_i^{exp} and pressure p_i^{exp} . The function f_1 represents the difference between the experimental and predicted saturated liquid density. The function f_2 is the difference between the liquid- and vapor-predicted chemical potentials. We have chosen this kind of function, as Müller and Gubbins (1996), instead of directly using the vapor pressure, since it allows us to obtain parameter values which not only provide a good fit of the experimental properties used as input but also provide a consistent vapor–liquid equilibrium diagram. To minimize the objective functions, the Marquart–Levenberg (Press et al., 1986) algorithm is used. The minimization process is finished when f_1 or f_2 are less than 10^{-6} .

For the case of binary mixtures, only two more adjustable parameters are needed to characterize the system. We have used Lorentz–Berthelot combining rules in the form given by eqs 15 and 16, with $\eta_{11} = \eta_{22} = 1$, $\eta_{12} = \eta_{21}$, $\xi_{11} = \xi_{22} = 1$, and $\xi_{12} = \xi_{21}$. The adjustable parameters to find are η_{12} and ξ_{12} . Although for some of the systems studied here the deviation of the 1–2-covolume from the arithmetic mean of the covolume of the pure substances is negligible, and hence we could consider $\eta_{12} = 1$, we have used both parameters as adjustable for all systems. The fitting procedure is carried out in the same way as that for pure substances.

Table 1. Parameter Values of Some Molecules of the n -Alkanes Series

substance	σ (nm)	$\epsilon_{\text{LJ}}/K_{\text{B}}$ (K)	m
methane	0.3722	147.3020	1.0000
ethane	0.3585	190.3750	1.5936
propane	0.3657	207.9678	1.9969
n -butane	0.3817	230.4479	2.1819
n -heptane	0.3697	240.1248	3.7256
n -octane	0.3787	249.8109	3.9476

The functions defined are

$$f_1(\sigma, \epsilon, m, \epsilon^{\text{HB}}, k^{\text{HB}}) = \sum_{i=1}^N \{x_i^{\text{exp}} - x_i^{\text{calc}}(p_i^{\text{exp}}, T_i^{\text{exp}})\}^2 \quad (19)$$

$$f_2(\sigma, \epsilon, m, \epsilon^{\text{HB}}, k^{\text{HB}}) = \sum_{i=1}^N \{y_i^{\text{exp}} - y_i^{\text{calc}}(p_i^{\text{exp}}, T_i^{\text{exp}})\}^2 \quad (20)$$

No additional parameters are needed to predict the phase equilibria of ternary systems.

Results

We have applied the soft-SAFT EOS to calculate the phase equilibria diagrams of pure and multicomponent fluids. Results can be divided in three groups: pure fluids, binary mixtures, and ternary mixtures. Temperature is presented in Kelvin, pressure in MPa, and molecular density in mol/dm³.

Pure Fluids

A. n -Alkanes. The accuracy of the equation is checked by correlating one of the simpler and more important chemical families, the n -alkane series. According to our model, n -alkanes need three molecular parameters, σ , ϵ , and m , to describe all thermodynamic properties.

These molecular parameters are calculated by fitting to the experimental saturated liquid density and equating the chemical potentials in both phases.

We have obtained the parameters for methane, ethane, propane, n -butane, and n -octane. We have fitted σ , ϵ , and m , except for methane, in which m was set to 1 (see Table 1). Figure 2 shows the results of the fitting for the coexistence curves. Symbols correspond to experimental results taken from Smith and Srivastava (1986a) while the solid lines are the results of the SAFT equation used in this work. SAFT gives excellent results over practically the whole range of density and temperature studied.

Vapor pressures as a function of temperature are shown in Figure 3. The top symbol of the different curves represents the experimental critical point, and the end lines are the predicted critical points. Note that SAFT is able to predict the anomalous behavior of the critical pressure of methane. Predictions in Figure 3a do not seem to be as good as the corresponding coexistence curves in Figure 2. This may be due to the fact that we have not fitted directly to the vapor pressure curve, but equated chemical potentials in both phases. Figure 3b provides an additional Clausius–Clapeyron plot, showing an excellent agreement between predictions and experimental results at low and moderate temperatures for all the substances studied.

One of the most promising results of applying SAFT to these systems is that, as seen with other versions of

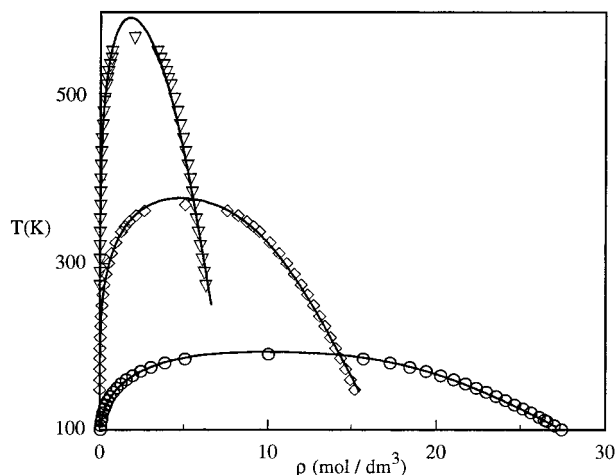


Figure 2. The coexistence curves of methane, propane, and *n*-octane. Solid lines are predictions from the SAFT EOS, and circles (methane), diamonds (propane), and triangles down (*n*-octane) represent the experimental points. The symbols at the top of the curves are the experimental critical points.

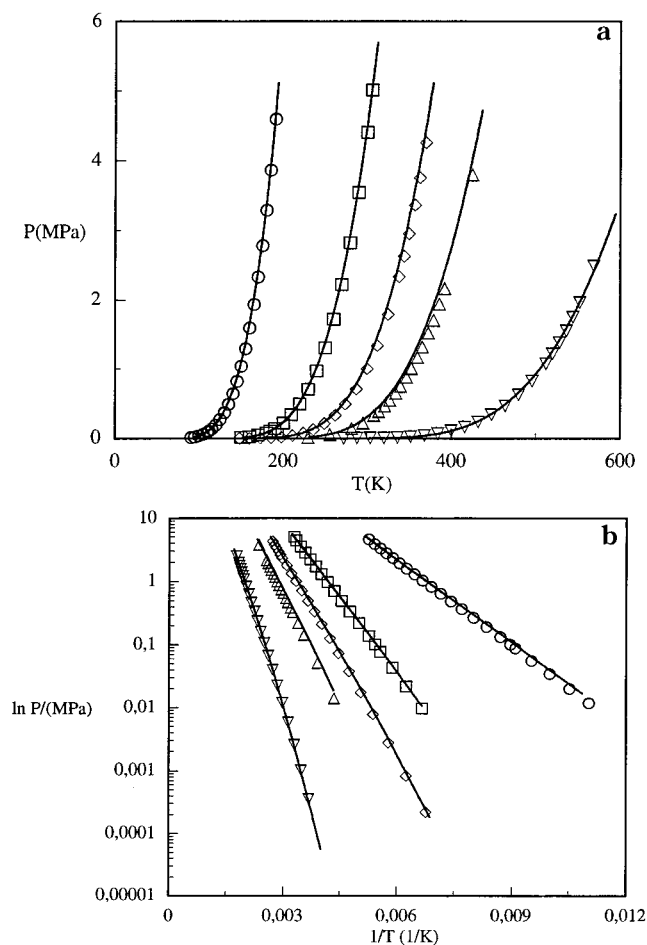


Figure 3. Vapor pressure curves (a) and Clausius-Clapeyron plot (b) for some members of the *n*-alkane series. Solid lines represent results from SAFT and circles (methane), squares (ethane), diamonds (propane), triangles up (*n*-butane), and triangles down (*n*-octane) correspond to experimental results. The curve at the lowest temperature corresponds to the methane, and the curve at highest temperature corresponds to the *n*-octane. The end lines represent the critical point predicted by the equation and the last symbols correspond (at highest temperature) to the experimental critical point.

SAFT (Fu and Sandler, 1995; Galindo et al., 1996, 1997), the molecular parameters increase linearly with mo-

lecular weight. The fact that transferable parameters can be obtained for a chemical family makes SAFT even more attractive, since it is able to predict not only multicomponent systems from pure fluids but also the thermodynamic behavior of pure systems that may be difficult to obtain experimentally. From a least squares analysis we find that the equations relating the molecular parameters with molecular weight are

$$m = 0.0306M_w + 0.5785 \quad (21)$$

$$m\sigma^3 = 0.0016M_w + 0.0246 \quad (22)$$

$$m\epsilon = 8.5532M_w + 26.7678 \quad (23)$$

These correlations are plotted in Figure 4. We have checked eqs 21–23 for the alkane series, from methane to nonane. Although the parameters estimated from these equations are not exactly the same as those given in Table 1, the phase envelopes and vapor pressures predicted from these parameters become indistinguishable from those obtained when fitting for members of the series with more than three carbons. In Figure 5 we compare experimental results for the coexistence curve of *n*-nonane to predictions made from SAFT using parameters estimated from these equations, instead of fitting. The agreement between the predicted and the observed behavior is excellent.

It should be noted that the ϵ equation (eq 23) gives the linear dependence of $m\epsilon$ with M_w , not just ϵ . The value of ϵ for different members of the *n*-alkane series is shown in Table 1. It is observed that the dispersive energy parameter strongly increases with the number of carbon atoms for the low members of the series. However, the addition of a new methyl group in the chain, for longer chains, does not essentially modify the structure of the molecule, and thus, the dispersive energy of the segments of the new *n*-alkane molecule should be nearly equal to that of the old chain. This is observed when the dispersive energy parameter is plotted against molecular weight: an asymptotic behavior of ϵ is seen when the number of carbon atoms increases. Hence, this EOS can be used with confidence for asymmetric mixtures, such as methane + C₄₀ or solvent + polymer (see also Blas and Vega, 1997).

B. 1-Alkenes. We have used the same equation to study some of the molecules of the 1-alkenes series. These substances are linear hydrocarbons not branched, with a nonsaturated bond between the first and the second carbon atom, and the rest of the bonds are saturated.

We choose to model these molecules as homonuclear chains. The phase equilibria has been calculated using the same procedure as for the *n*-alkanes, obtaining the three molecular parameters, σ , ϵ , and m . Since these are effective molecular parameters and we use the same molecular model as for *n*-alkanes, their numerical values are slightly different than those for the corresponding alkane molecule. Parameters obtained from the fitting are presented in Table 2. Figure 6 shows the liquid-vapor diagrams for these systems. Lines correspond to the SAFT results and symbols are the experimental results taken from Smith and Srivastava (1986a). The vapor pressure as functions of the temperature over the fitted range are presented in Figure 7. Figure 7a represents a traditional plot of the vapor pressure versus temperature, while Figure 7b is a

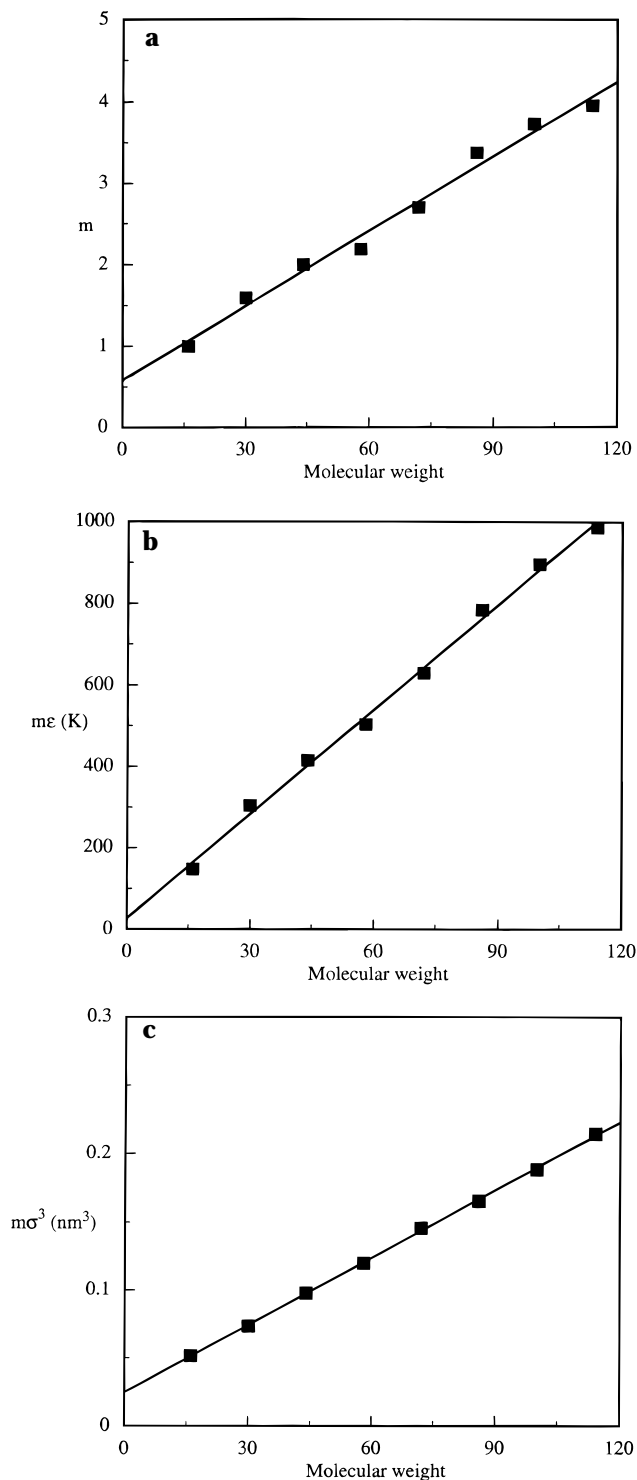


Figure 4. Transferable parameters of the SAFT EOS for the series of *n*-alkanes, correlated from methane to *n*-octane. (a) Chain length as a function of the molecular weight. (b) $m\epsilon$ as a function of the molecular weight. (c) $m\sigma^3$ as a function of the molecular weight.

Clausius–Clapeyron plot to highlight the agreement between predictions and experimental results at the region of low and moderate temperatures. The top symbols correspond to the experimental critical point, and the end lines represent the critical point predicted by the soft-SAFT EOS. As for the alkane series, the agreement between SAFT and experimental results is remarkable for all members of the series, although critical pressures are overestimated, as expected.

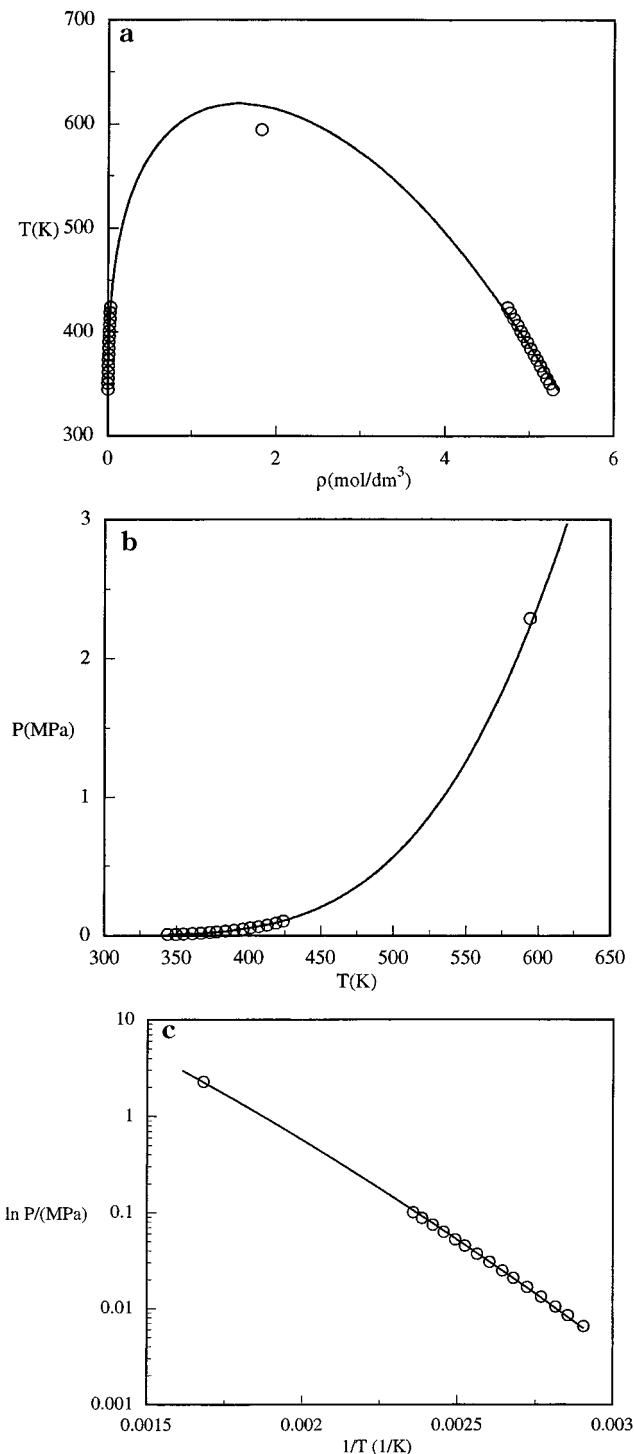


Figure 5. Comparison between experimental results (circles) and predictions from SAFT using the transferable parameters found in this work (solid lines) for the *n*-nonane system. (a) Coexistence curve. (b) Vapor pressure as a function of the temperature. (c) Clausius–Clapeyron plot.

Table 2. Parameter Values of Some Molecules of the 1-Alkenes Series

substance	σ (nm)	ϵ_{LJ}/K_B (K)	m
ethene	0.3372	170.092	1.7032
1-propene	0.3566	206.561	1.9681
1-butene	0.3762	228.796	2.1470
1-pentene	0.3737	233.582	2.6120

C. 1-Alkanols. To check the accuracy of the soft-SAFT equation to predict the behavior of associating fluids, the 1-alkanols series is studied following the

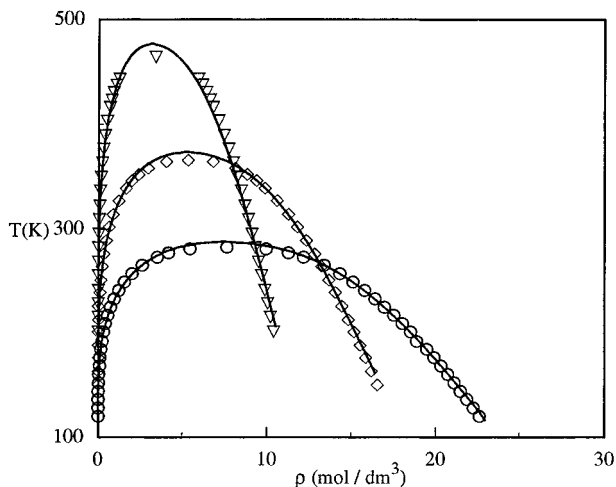


Figure 6. The coexistence curves of ethene, 1-propene, and 1-pentene. Solid lines are the predictions by the SAFT EOS, and circles (ethene), diamonds (1-propene), and triangles down (1-pentene) represent experiments taken from the literature. As in the previous figure, the points at the highest temperature are the critical points from experiments.

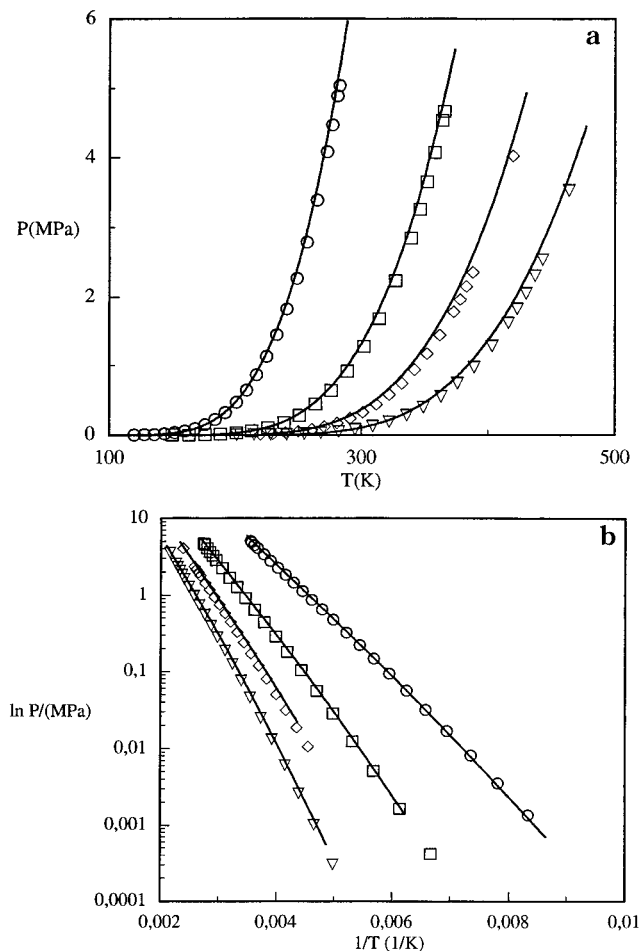


Figure 7. Vapor pressure curves (a) and Clausius-Clapeyron diagrams (b) for some 1-alkenes studied. Symbols are as in Figure 6. Curves are the predictions of the SAFT for different members of the series. The end lines are the predicted critical points and the top symbol on each correspond to the experimental critical points.

same procedure as for the *n*-alkane and 1-alkenes series. In addition to σ , ϵ , and m , two more adjustable parameters are needed in this case, namely, the volume and

Table 3. Parameter Values of Some Molecules of the 1-Alkanols Series

substance	σ (nm)	ϵ_{LJ}/K_B (K)	m	ϵ_{HB}/K_B (K)	k_{HB}
methanol	0.4021	214.992	0.9109	3671.516	52.012
ethanol	0.3887	233.227	1.4343	3600.672	41.280
1-propanol	0.3786	259.158	2.0059	3375.891	32.780
1-butanol	0.3959	279.897	2.1948	3519.281	22.082
1-octanol	0.4843	316.101	2.2334	4333.446	12.401

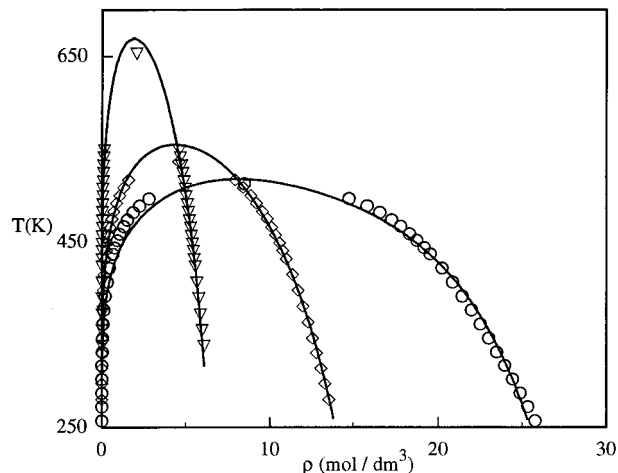


Figure 8. The coexistence curves of methanol (circles), 1-propanol (diamonds), and 1-octanol (triangles down). Solid lines are predictions from the SAFT equation used in this work and symbols correspond to experimental results.

energy of association. Parameters obtained for this series are presented in Table 3.

The coexistence lines for some of the 1-alkanols studied are shown in Figure 8. Symbols correspond to experimental results by Smith and Srivastava (1986b) while solid lines represent results from the soft-SAFT equation. Vapor pressures as a function of temperature are presented in Figure 9 (part a is the vapor pressure/temperature diagram and part b is the corresponding Clausius-Clapeyron plot). Again, as for the other two series studied, calculations using the soft-SAFT equation of state are in excellent agreement with experimental results.

Binary Mixtures

We present results for the systems methane/ethane/propane and ethane/*n*-butane/*n*-heptane. Before studying these systems, the binary parameters of the mixtures composing them need to be obtained. Although we have studied several binary mixtures, we will discuss only the results needed to predict the behavior of the ternary systems. The work we present here is focused on the application of soft-SAFT to binary and ternary mixtures of *n*-alkanes. The same equation can be applied to more complicated mixtures, that is, mixtures with associating and nonassociating components.

A. Methane/Ethane. The chain length of both substances are low and similar. The binary parameters (see eqs 15 and 16) are shown in Table 4. These values are obtained by fitting to experimental data for the molar fraction on the liquid and the vapor sides at $T = 172.04$ K. The rest of the curves are obtained using the pure parameters of the substances and the fitted values at this temperature. Note that the binary parameters ξ and η are independent of the thermodynamic conditions of study and explicitly do not depend on temperature and/or composition.

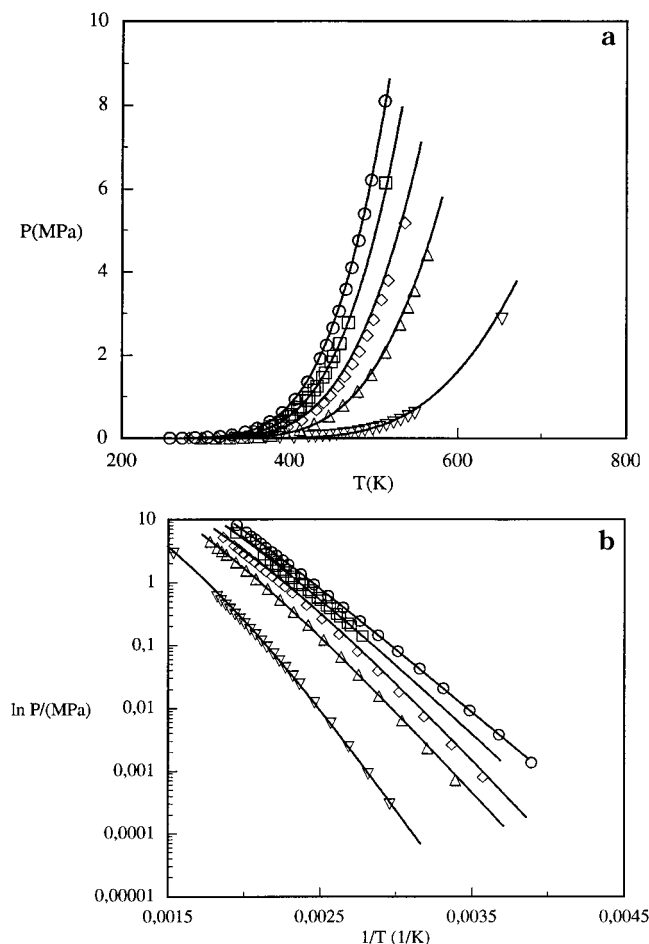


Figure 9. Vapor pressure curves (a) and Clausius-Clapeyron plot (b) for methanol, 1-propanol, and 1-octanol. Symbols as in Figure 8.

Table 4. Parameter Values of the Binary Mixtures

mixture	ξ	η
methane/ethane	0.9998	1.0219
methane/propane	0.9888	1.0246
ethane/propane	1.0031	1.0146
ethane/ <i>n</i> -butane	0.9838	1.0090
ethane/ <i>n</i> -heptane	0.9837	1.0238
<i>n</i> -butane/ <i>n</i> -heptane	1.0032	1.0241

The pressure/composition projection of the phase diagram for methane/ethane at three different temperatures is shown in Figure 10. Solid lines correspond to results from the SAFT equation used in this work and the symbols are experimental results taken from Wichterle and Kobayashi (1972a). All the temperatures studied are subcritical temperatures with respect to methane and ethane. Note that for $T = 158.15$ and 144.26 K the solid lines are predictions from SAFT and are not fitted. The agreement between predictions and experimental results is excellent over the whole range of composition.

B. Methane/Propane. The next binary mixture studied is the system methane/propane. Figure 11 shows the pressure/composition diagram at several temperatures. Different lines correspond to the predicted results and the symbols are the experimental results taken from Wichterle and Kobayashi (1972b). The three temperatures chosen are in the subcritical region of the methane and propane pure fluids. The temperature selected to fit the binary parameters (see Table 4) was $T = 172.04$ K as before. The rest of the

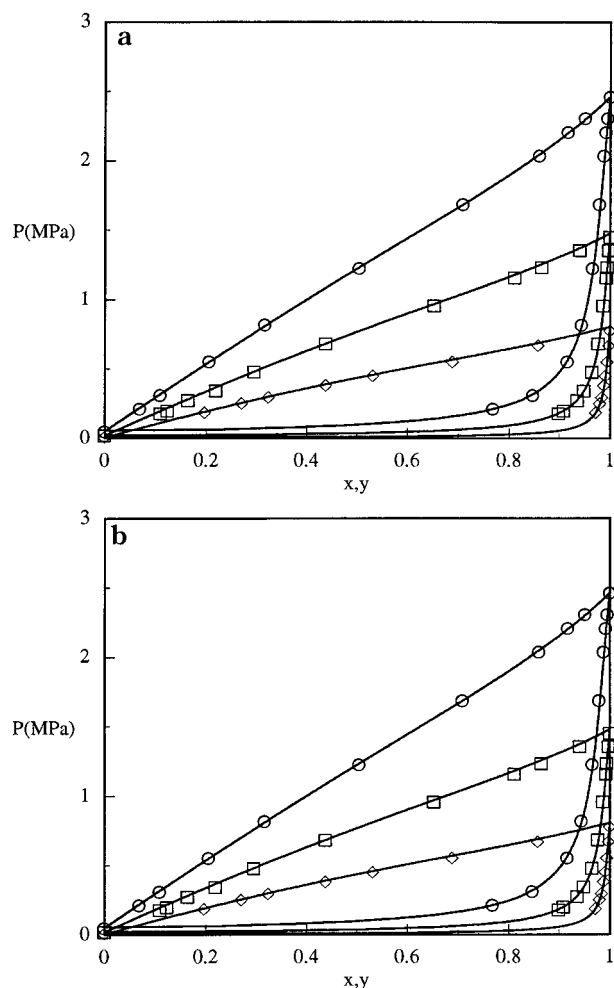


Figure 10. Pressure/composition diagrams for the methane/ethane mixture. Solid lines correspond to the predictions from the SAFT EOS and symbols represent the experimental results. Curves from high to low temperatures correspond to $T = 172.04$ K (circles), 158.15 K (squares), and 144.26 K (diamonds), respectively.

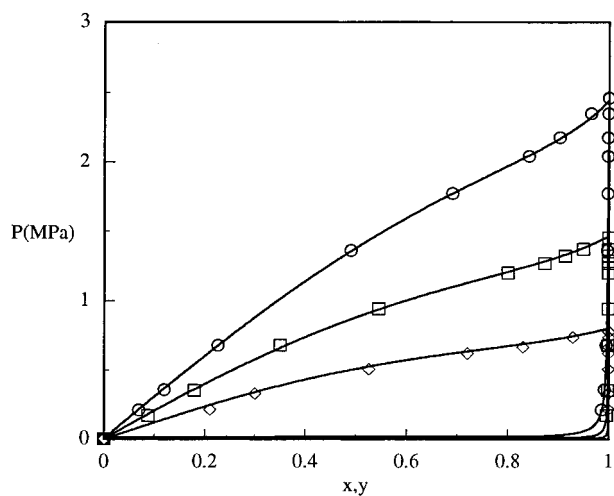


Figure 11. Pressure/composition diagrams for methane/propane mixtures. Legend as in Figure 10.

curves are predictions from these fitted parameters and the set of parameters for pure methane and pure propane (Table 1). As expected, results obtained from SAFT are in excellent agreement with the experimental results.

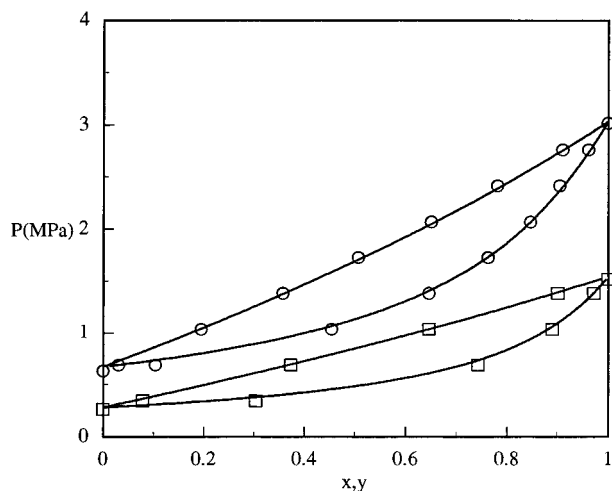


Figure 12. Pressure/composition diagrams for ethane/propane mixtures. Solid lines correspond to the predictions of the SAFT. Experimental results at $T = 283$ K are represented by circles and at $T = 255.33$ K by squares.

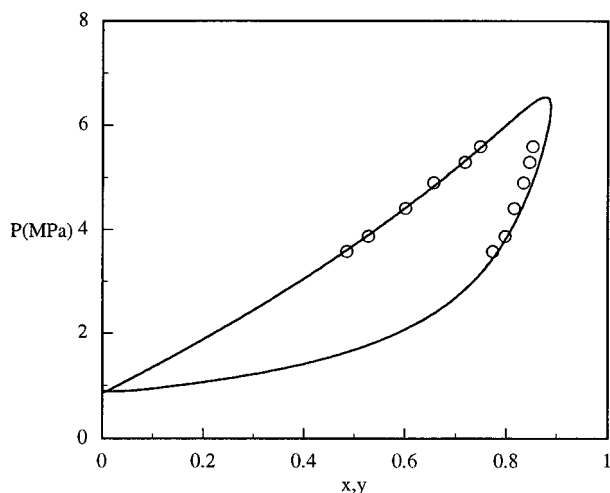


Figure 13. Pressure/composition diagram for ethane/*n*-butane mixture at $T = 338.65$ K. Solid line is the prediction of the SAFT (with $\xi_{12} = \eta_{12} = 1$), and circles are the experimental data.

C. Ethane/Propane. The pressure/composition diagram of the ethane/propane mixture at two different temperatures is shown in Figure 12. The solid lines are the predicted results from soft-SAFT and the symbols are the experimental results taken from Matschke and Thodos (1962). As in the previous mixtures, both temperatures are chosen to be subcritical for the pure components. We obtain the binary parameters of the mixture (Table 4) by fitting at $T = 283$ K. The other solid line corresponds to predictions by SAFT at $T = 255.33$ K. The agreement between predictions and experimental results is remarkable, even in the proximity of the pure component regions.

To check the validity of SAFT to predict ternary diagrams of components differing in size (chain length in our case), we have chosen the system ethane/*n*-butane/*n*-heptane. To investigate this system another set of binary mixtures need to be studied first: ethane/*n*-butane, ethane/*n*-heptane, and *n*-butane/*n*-heptane.

D. Ethane/*n*-Butane. Predictions from SAFT for this mixture from the pure component parameters are shown in Figure 13 for $T = 338.65$ K. In this case the binary parameters are set equal to unity. Although the general agreement is quite good, it can be improved by

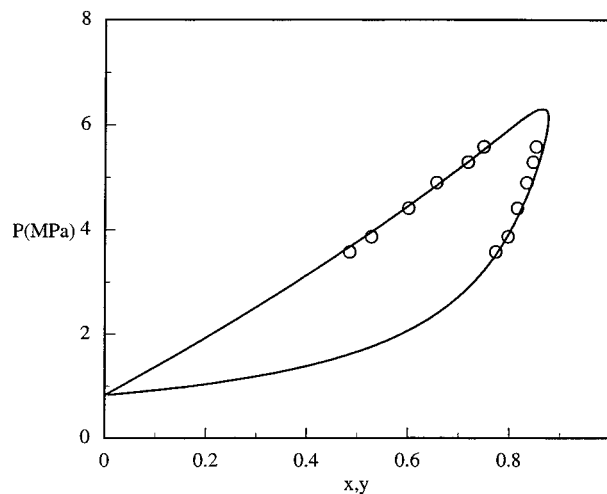


Figure 14. Pressure/composition diagram for ethane/*n*-butane mixture at $T = 338.65$ K. Solid line is the adjustment of the SAFT and circles represent the experimental data.

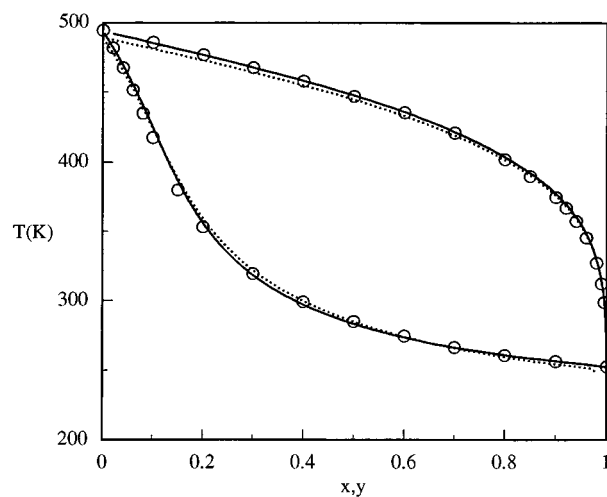


Figure 15. Comparison between results from SAFT and experimental results for the ethane/*n*-heptane binary mixture at $P = 1.379$ MPa. Dotted line corresponds to the predictions (binary parameters set equal to 1), the solid line corresponds to the best fitting, and circles are the experimental data for this system.

fitting as we did with the previous binary mixtures studied. The objective of this fitting is to obtain the best possible parameters to predict the ternary mixtures. The optimal fit is obtained when $\xi_{12} = 0.9838$ and $\eta_{12} = 1.0090$ and is shown in Figure 14. Experimental results are taken from Mehra and Thodos (1965).

E. Ethane/*n*-Heptane. Figure 15 shows the predictions made by SAFT from the pure component parameters for the mixture ethane/*n*-heptane at $P = 1.379$ MPa. A slightly better prediction can be obtained when adjusting the binary parameters (see Table 4), as shown in Figure 16. Experimental results from Kay (1938) are represented by symbols. Predictions of SAFT are shown with lines: the dotted line corresponds to predictions from the pure component parameters, while the solid line comes from the fitting at this pressure. These fitted binary parameters are used to predict the behavior of the mixture at a lower pressure, $P = 0.689$ MPa. Again, the agreement between the predicted values and the experimental results is excellent.

F. *n*-Butane/*n*-Heptane. The last binary mixture studied corresponds to *n*-butane/*n*-heptane. In Figure

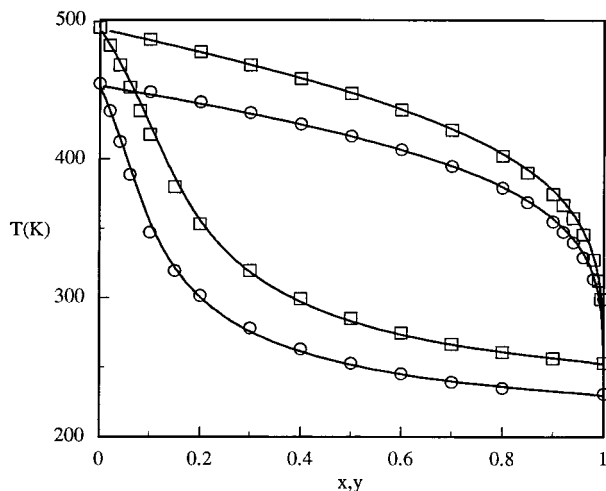


Figure 16. Temperature/composition diagrams for the ethane/*n*-heptane mixture. Solid lines correspond to the predictions of the SAFT and symbols are the experimental data at $P = 0.689$ MPa (circles) and $P = 1.379$ MPa (squares).

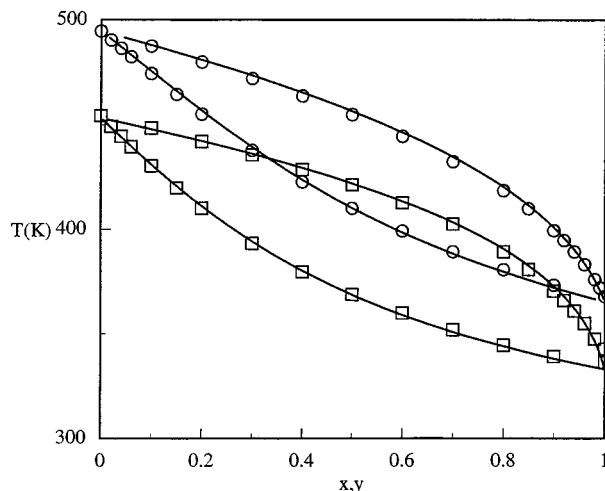


Figure 18. Temperature/composition diagrams for *n*-butane/*n*-heptane system at different pressures. Solid lines represent the SAFT results and symbols are experimental results at $P = 0.689$ MPa (squares) and $P = 1.379$ MPa (circles).

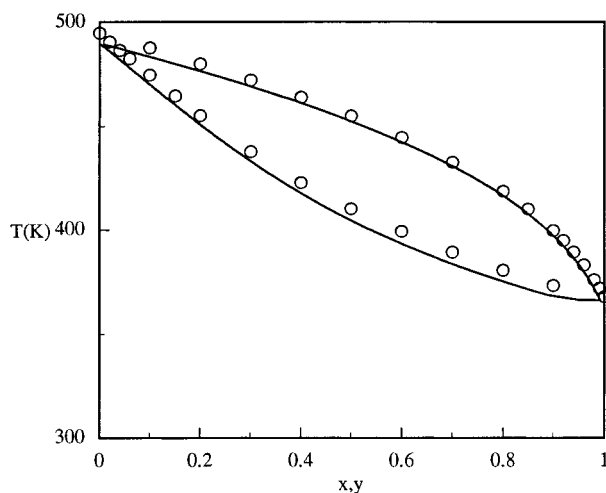


Figure 17. Temperature/composition diagram for the *n*-butane/*n*-heptane binary mixture. Solid line is the prediction of the equation of state (setting the binary parameters to unity) and circles are the experimental points. The pressure is equal to 1.379 MPa.

17 we show a comparison between experimental results (Kay, 1941) for this system at $P = 1.379$ MPa and predictions from SAFT using the pure component parameters, that is, fixing $\xi_{12} = \eta_{12} = 1.0$. Although predictions are quite good without any further adjustment, we decided to fit the binary parameters as in the previous cases, for the ternary system study. In Figure 18 we show the comparison between the SAFT correlation for this mixture and the experimental results for the optimal binary parameters, $\xi_{12} = 1.0032$ and $\eta_{12} = 1.0241$. These parameters are used to predict the behavior of the mixture at $P = 0.689$ MPa, as shown in the same figure.

Ternary Mixtures

To test the accuracy of SAFT in predicting ternary diagrams, we investigate *n*-alkane mixtures of two systems at different thermodynamic conditions. Since the molecular parameters have a clear physical meaning and the binary parameters have predicted accurately the phase behavior of the binary mixtures at different conditions from which they were calculated, the equa-

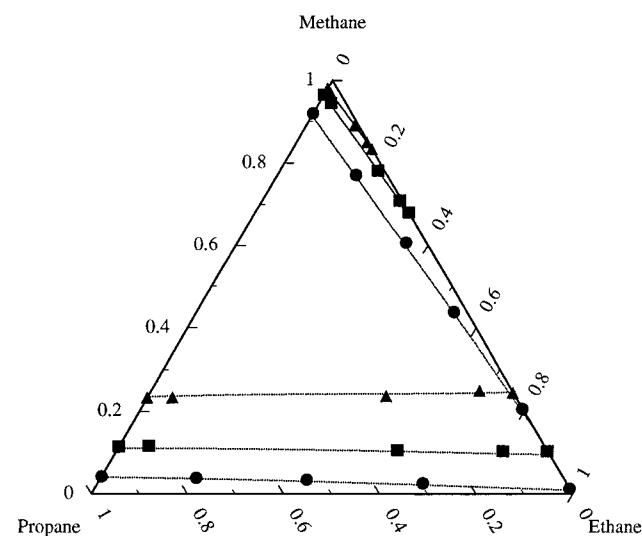


Figure 19. Ternary-phase diagram for methane/ethane/propane. Different lines correspond to the predictions from the soft-SAFT EOS and symbols are the experimental results at $T = 199.82$ K. Circles correspond to pressure equal to 0.276 MPa, squares to 0.689 MPa, and triangles to 1.379 MPa.

tion is expected to accurately predict the ternary diagrams without any further fitting. We choose a system of similar components: methane/ethane/propane and a second system where components have different chain length, ethane/*n*-butane/*n*-heptane. The shape of the coexistence curve as well as the tie lines are discussed in detail.

A. Methane/Ethane/Propane. The binary parameters obtained for the methane/ethane, methane/propane, and ethane/propane mixtures (Table 4) are used in conjunction with the molecular parameters of the pure components (Table 1) to predict the phase behavior of this ternary system.

The ternary composition diagrams of this mixture at different pressures and a fixed temperature of 199.83 K are shown in Figures 19 and 20. Experimental results are taken from Wichterle and Kobayashi (1972c) and are represented by symbols. The solid lines correspond to predictions made by the soft-SAFT equation. Different symbols correspond to different pressures, from 0.276 to nearly 5 MPa. The experimental data

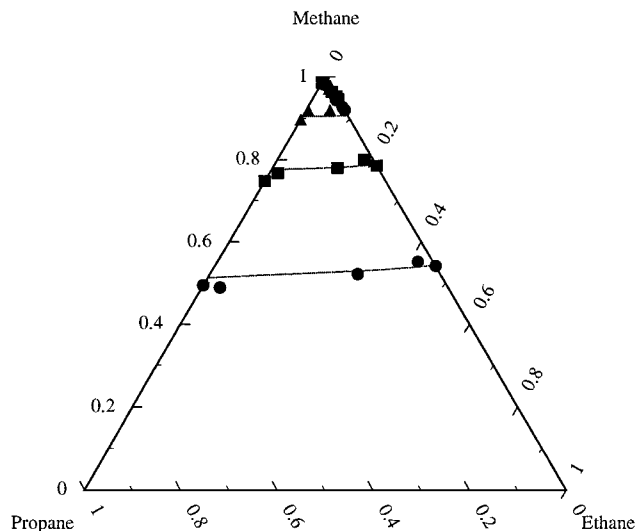


Figure 20. Ternary-phase diagram for the methane/ethane/propane mixture. Different lines correspond to the SAFT predictions and symbols are the experimental results at $T = 199.82$ K. Circles correspond to pressure equal to 2.758 MPa, squares to 4.137 MPa, and triangles to 4.999 MPa.

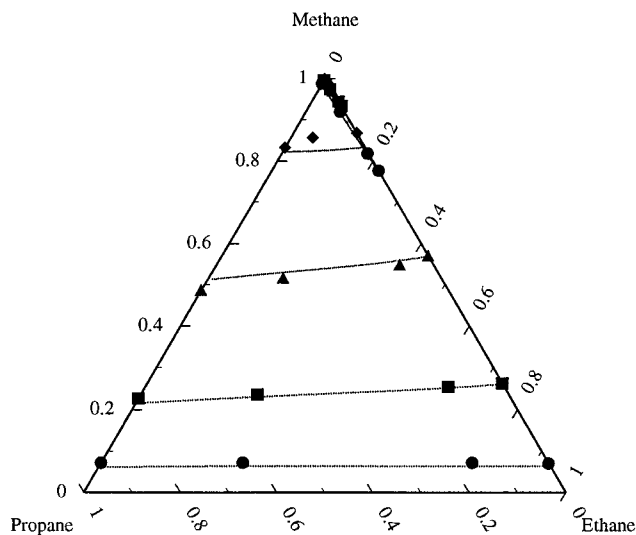


Figure 21. Ternary-phase diagram for the methane/ethane/propane system. Predictions from SAFT are represented by solid lines and symbols correspond to experimental data at $T = 172.04$ K. Circles represent $P = 0.221$ MPa, squares $P = 0.69$ MPa, triangles $P = 1.379$ MPa, and rhombus $P = 2.068$ MPa.

used are distributed over the whole concentration range of the ternary mixture.

The overall agreement between SAFT and experimental results is excellent. In the low-pressure region, the liquid and vapor sides are correctly predicted. When the pressure is increased, the agreement between predictions and experimental results deteriorates, probably due to the proximity of the critical point of methane. It should be noted that in all cases studied the molar fractions predicted deviate from experiments by less than 5%.

The mixture is also studied at a lower temperature, $T = 172.04$ K, and different pressures, from 0.221 to 2.068 MPa, as shown in Figure 21. The solid lines correspond to predictions of the equation of state and the symbols are the experimental points taken from the literature (Wichterle and Kobayashi, 1972c). The agreement between results from experiments and predictions is excellent.

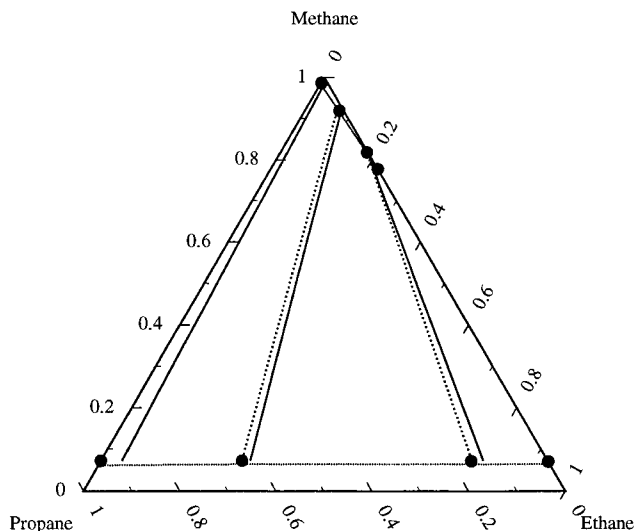


Figure 22. Phase diagram showing tie lines of the system methane/ethane/propane at $T = 172.04$ K and $P = 0.221$ MPa. Solid lines represent the SAFT predictions and experimental points are represented by circles. Experimental tie lines are shown as dotted lines while solid lines connecting the equilibrium points are the tie lines predicted by SAFT.

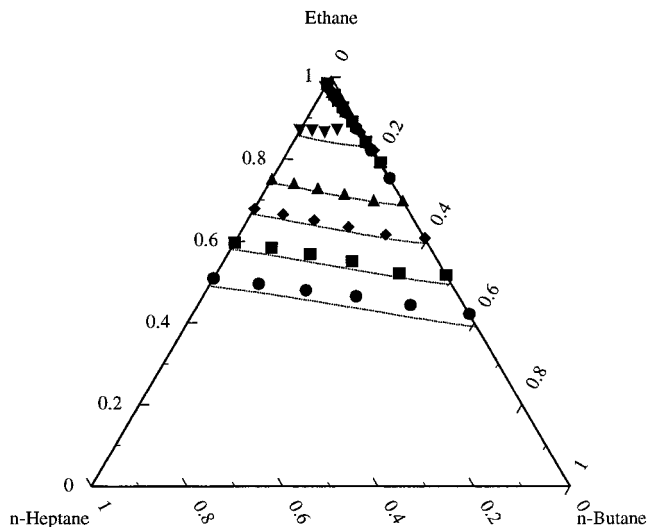


Figure 23. Ternary-phase diagram for the ethane/*n*-butane/*n*-heptane system at $T = 338.71$ K. Solid lines correspond to the predictions from SAFT at different pressures and symbols are experimental results at $P = 3.103$ MPa (circles), 3.792 MPa (squares), 4.482 MPa (rhombus), 5.171 MPa (triangles up), and 6.343 MPa (triangles down).

In Figure 22 we represent the phase diagram for methane/ethane/propane at $T = 172.04$ K and $P = 0.221$ MPa where the tie lines connecting the equilibrium points are shown for the experimental and predicted results. It is seen not only that SAFT is able to predict the shape of the curve but also that the tie lines obtained from SAFT and the experimental tie lines are parallel in all cases.

B. Ethane/*n*-Butane/*n*-Heptane. A more challenging system to study is one in which the components are more different. We have chosen to check the accuracy of the equation for the ternary mixture ethane/*n*-butane/*n*-heptane. Soft-SAFT is applied in the same way as for the other ternary systems: molecular parameters of the pure components are taken from Table 1 and binary parameters from Table 4. A comparison between predicted and experimental phase diagrams of this

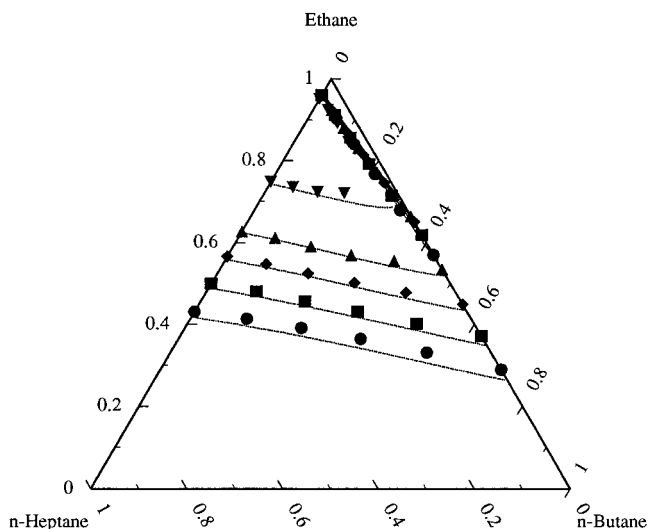


Figure 24. Ternary diagram for the ethane/*n*-butane/*n*-heptane mixture at $T = 366.48$ K. Solid lines are results from SAFT and symbols are experimental data at 3.447 MPa (circles), 4.137 MPa (squares), 4.826 MPa (rhombus), 5.516 MPa (triangles up), and 6.895 MPa (triangles down).

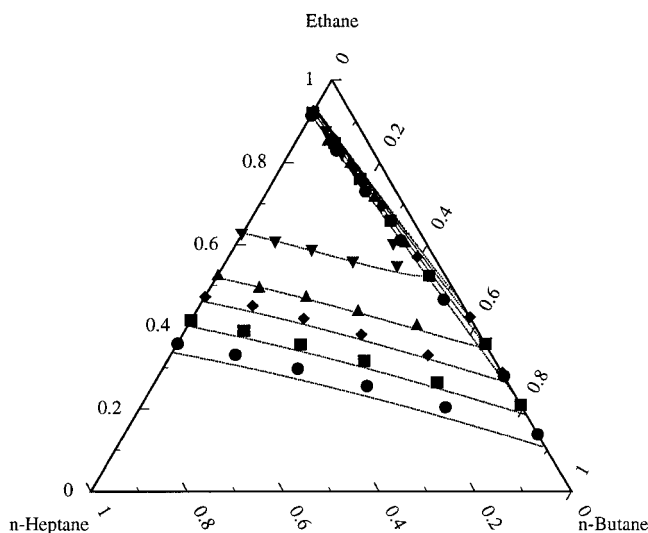


Figure 25. Ternary-phase diagram for the ethane/*n*-butane/*n*-heptane at $T = 394.26$ K. Legend as in Figure 24.

mixture at $T = 338.71$, 366.48, and 394.26 K is shown in Figures 23–25. Again, symbols correspond to experimental results taken from the literature (Mehra and Thodos, 1966), while solid lines correspond to SAFT results.

Since from these figures it may not be clear how well SAFT does for a particular set of conditions, in Figure 26 we plot the comparison between SAFT (solid lines) and experimental results (symbols) for $T = 394.26$ K and $P = 4.826$ MPa. Tie lines from the equation are represented by solid lines, while experimental tie lines are plotted with dotted lines. Again, the agreement between predicted and experimental results is excellent.

Once SAFT has proven to be a reliable equation for these mixtures compared to experimental results, it can be used to predict the behavior of the systems at conditions at which experiments may be hard or impossible to perform. In Figure 27 we show predictions from SAFT for the mixture ethane/*n*-butane/*n*-heptane at $T = 477.59$ K and three pressures, represented by different lines.

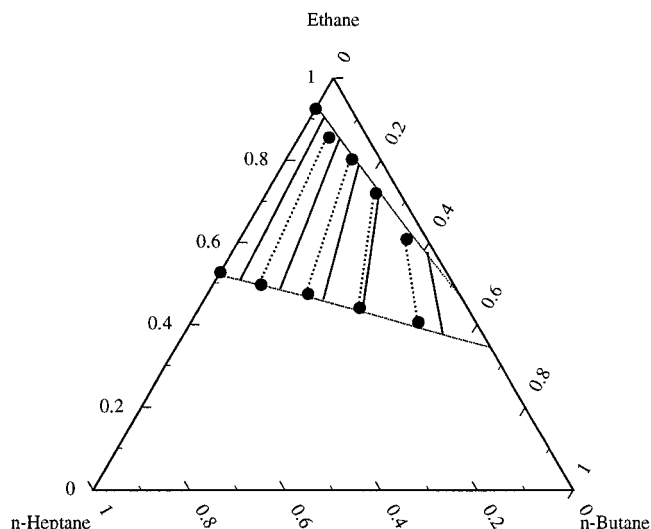


Figure 26. Phase diagram showing tie lines of the system ethane/*n*-butane/*n*-heptane at $T = 394.26$ K and $P = 4.826$ MPa. Legend as in Figure 22.

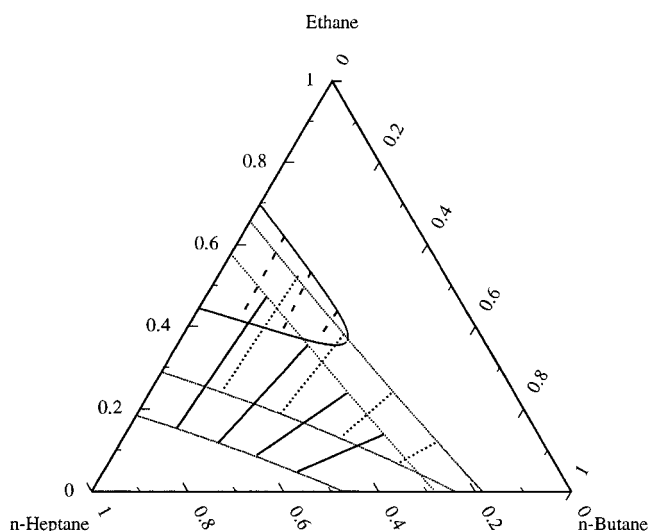


Figure 27. Predictions from the soft-SAFT equation for the ethane/*n*-butane/*n*-heptane system at $T = 477.59$ K. Different solid lines correspond to pressures equal to 4.137, 5.516, and 8.274 MPa from low to high molar fractions of *n*-heptane. Tie lines of these coexistence curves are also shown.

Conclusions

The soft-SAFT EOS has been applied to correlate some compounds of the homologous series of *n*-alkanes, 1-alkenes, and 1-alkanols. We have found transferable molecular parameters for the *n*-alkane series. Only three molecular parameters are needed for pure hydrocarbons to obtain all thermodynamic properties of the system. For the case of associating molecules two additional parameters are needed.

The same equation has been used to correlate binary mixtures of hydrocarbons adjusting two parameters, which do not depend on temperature and/or composition. Molecular parameters have been used in conjunction with these binary parameters to successfully predict the behavior of the binary mixtures at different thermodynamic conditions and the behavior of ternary mixtures.

The equation has proven to be excellent in predicting the behavior of multicomponent systems from molecular parameters (pure components) and just two binary

parameters. It correctly predicts the phase envelope of binary and ternary mixtures as well as the tie lines connecting the equilibrium points.

Acknowledgment

It is a pleasure to thank Professors Keith E. Gubbins and Allan Mackie for helpful discussions. Comments from the anonymous referees are also gratefully acknowledged. This work was supported by Projecte de Nova Implantació no. URV95-GNI-05 and the DGICyT (PB96-1025). One of us (F.J.B.) has a doctoral fellowship from Comisionat per a Universitats i Recerca from the Generalitat de Catalunya. The financial support of this fellowship is gratefully acknowledged.

Nomenclature

ϕ_{LJ} = Lennard–Jones potential energy
 σ_{ij} = segment size between molecules i and j
 ϵ_{ij} = dispersive energy between molecules i and j
 r_{ij} = intermolecular distance
 ϵ_{HB} = association energy
 σ^{HB} = associating site size
 r_{AB} = distance between two associating sites
 A^{ideal} = ideal Helmholtz free energy
 A^{LJ} = Lennard–Jones Helmholtz free energy
 A^{chain} = chain Helmholtz free energy
 A^{assoc} = associating Helmholtz free energy
 k_B = Boltzmann constant
 T, T^* = temperature, reduced temperature
 N_m = number of molecules
 x_i = chain molar fraction of component i
 X_i = segment molar fraction of component i
 $N_m^{(i)}$ = number of molecules type i
 Λ_i = thermal de Broglie wavelength
 ρ_m, ρ^* = total molecular density, reduced monomeric density
 $\rho_m^{(i)}$ = molecular density of chain i
 m_i = chain length of species i
 n = number of components
 $g_R^{LJ}(\sigma)$ = radial distribution function of the reference fluids (Lennard–Jones)
 a_{ij} = constant for the $g_R^{LJ}(\sigma)$ expression
 p, p^R = pressure, pressure of the reference fluid
 $X_A^{(i)}$ = fraction of nonbonded molecules i at the associating site A
 $n(\Gamma^{(i)})$ = number of associating sites in the component i
 $g_{LJ}^{(ik)}(\sigma)$ = reference fluid correlation function
 $\Delta_{AB}^{(ik)}$ = measure of the strength and volume interaction between sites A and B
 $f_{AB}^{(ik)}(12)$ = Mayer f function between the associating sites A and B, in the molecules 1 and 2, of species i and k , respectively
 ϵ_{AB}^{HB} = hydrogen bond energy between the associating sites A and B
 I = integral involving the geometry of the associating sites
 r^* = reduced distance
 $f_{AB}^{(ik)}$ = Mayer f function for the associating interaction between sites A and B of molecules i and k , respectively
 k_{HB} = volume of interaction of hydrogen bond
 σ_m = segment size of the hypothetical fluid to model the mixture
 ϵ_m = dispersive energy of the hypothetical fluid to model the mixture
 $g_m(r^*, \rho_m^*, T_m^*)$ = radial distribution function of the Lennard–Jones fluid as a function of distance, density, and temperature
 η_{ij}, ξ_{ij} = parameters for the Lorentz–Berthelot combining rules

p^I, p^{II} = pressure at phases I and II
 $\mu^I, \mu^{II}, \mu_1^I, \mu_2^{II}$ = chemical potentials at phases I and II, and chemical potentials of components 1 and 2 at phases I and II
 ρ^I, ρ^{II} = coexistence densities at phases I and II
 x^I, x^{II} = molar fractions at I and II

Superscripts

assoc = association
 ideal = ideal gas
 chain = chain term
 ref = reference
 $i, 1, 2, \dots$ = type of molecules
 $*$ = reduced units
 HB = hydrogen bond
 I, II = phases

Subscripts

$i, j, 1, 2, \dots$ = type of molecules
 m = molecular property
 A, B, ... = associating sites

Literature Cited

- Amos, M. D.; Jackson, G. BHS Theory and Computer Simulations of Linear Heteronuclear Triatomic Hard-Spheres Molecules. *Mol. Phys.* **1991**, *74*, 191.
- Archer, A. L.; Jackson, G. Theory and Computer Simulations of Heteronuclear Diatomic Hard-Spheres Molecules (Hard Dumbbells). *Mol. Phys.* **1991**, *73*, 881.
- Banaszak, M.; Chiew, Y. C.; Radosz, M. Thermodynamic Perturbation Theory: Sticky Chains and Square-Well Chains. *Phys. Rev. E* **1993**, *48*, 3760.
- Banaszak, M.; O'Lenick, R.; Chiew, Y. C.; Radosz, M. Thermodynamic Perturbation Theory: Lennard-Jones Chains. *J. Chem. Phys.* **1994**, *100*, 3803.
- Banaszak, M.; Chen, C. K.; Radosz, M. Copolymer SAFT Equation of State. Thermodynamic Perturbation Theory Extended to Heterobonded Chains. *Macromolecules* **1996**, *29*, 6481.
- Blas, F. J.; Vega, L. F. Thermodynamic Behavior of Homonuclear and Heteronuclear Lennard-Jones Chains with Association Sites from Theory and Simulation. *Mol. Phys.* **1997**, in press.
- Bokis, C. P.; Donohue, M. D. A Closed-Form Equation of State for Lennard-Jones Molecules Based on Perturbation Theory. *J. Phys. Chem.* **1995**, *99*, 12655.
- Chang, J.; Sandler, S. I. An Equation of State for the Hard-Sphere Chain Fluid: Theory and Monte Carlo Simulation. *Chem. Eng. Sci.* **1994**, *49*, 2777.
- Chapman, W. G. Prediction of the Thermodynamic Properties of Associating Lennard-Jones Fluids: Theory and Simulation. *J. Chem. Phys.* **1990a**, *93*, 4299.
- Chapman, W. G. Theory and Simulation of Associating Liquid Mixtures. Ph.D. Dissertation, Cornell University, Ithaca, NY, 1990b.
- Chapman, W. G.; Jackson, G.; Gubbins, K. E. Phase Equilibria of Associating Fluids: Chain Molecules with Multiple Bonding Sites. *Mol. Phys.* **1988**, *65*, 1057.
- Chapman, W. G.; Gubbins, K. E.; Jackson, G.; Radosz, M. New Reference Equation of State for Associating Liquids. *Ind. Eng. Chem. Res.* **1990**, *29*, 1709.
- Chen, S. S.; Kreglewski, A. Applications of the Augmented van der Waals Theory of Fluids. I. Pure Fluids. *Ber. Bunsen-Ges. Phys. Chem.* **1977**, *81*, 1048.
- Economou, I. G.; Donohue, M. D. An Equation of State with Multiple Associating Sites for Water and Water-Hydrocarbon Mixtures. *Ind. Eng. Chem. Res.* **1992**, *31*, 2388.
- Economou, I. G.; Tsonopoulos, C. Associating Models and Mixing Rules in Equations of State for Water/Hydrocarbon Mixtures. *Chem. Eng. Sci.* **1997**, *52*, 511.
- Fu, Y.-H.; Sandler, S. I. A Simplified SAFT Equation of State for Associating Compounds and Mixtures. *Ind. Eng. Chem. Res.* **1995**, *34*, 1897.
- Galindo, A.; Whitehead, P. J.; Jackson, G.; Burgess, A. N. Predicting the High-Pressure Phase Equilibria of Water +

- n*-Alkanes Using a Simplified SAFT Theory with Transferable Intermolecular Interaction Parameters. *J. Phys. Chem.* **1996**, *100*, 6781.
- Galindo, A.; Whitehead, P. J.; Jackson, G.; Burgess, A. N. Predicting the Phase Equilibria of Mixtures of Hydrogen Fluoride with Water Difluoromethane (HFC-32), and 1,1,1,2-Tetrafluoroethane (HFC-134a) Using a Simplified SAFT Approach. *J. Phys. Chem. B* **1997**, *101*, 2082.
- Georgoulaki, A. M.; Ntoulos, I. V.; Panagiotopoulos, A. Z.; Tassios, D. P. Phase Equilibria of Binary Lennard-Jones Mixtures: Simulation and Conformal Solutions Theory. *Fluid Phase Equilib.* **1994**, *100*, 153.
- Ghonasgi, D.; Chapman, W. G. Theory and Simulation for Associating Fluids with Four Bonding Sites. *Mol. Phys.* **1993a**, *79*, 291.
- Ghonasgi, D.; Chapman, W. G. Theory and Simulation for Associating Chain Fluids. *Mol. Phys.* **1993b**, *80*, 161.
- Ghonasgi, D.; Chapman, W. G. Prediction of the Properties of Model Polymer Solutions and Blends. *AIChE J.* **1994a**, *40*, 878.
- Ghonasgi, D.; Chapman, W. G. Theory and Simulation for Associating Hard Chain Fluids. *Mol. Phys.* **1994b**, *83*, 145.
- Ghonasgi, D.; Chapman, W. G. A New Equation of State for Hard Chain Molecules. *J. Chem. Phys.* **1994c**, *100*, 6633.
- Gil-Villegas, A.; Galindo, A.; Whitehead, P. J.; Mills, S. J.; Jackson, G. Statistical Associating Fluid Theory for Chain Molecules with Attractive Potentials of Variable Range. *J. Chem. Phys.* **1997**, *106*, 4168.
- Gupta, R. B.; Johnston, K. P. Lattice Fluid Hydrogen Bonding Model with a Local Segment Density. *Fluid Phase Equilib.* **1994**, *99*, 135.
- Hansen, J. P.; McDonald, I. R. *Theory of Simple Liquids*; Academic Press: New York, 1990.
- Harismiadis, V. I.; Koutras, N. K.; Tassios, D. P.; Panagiotopoulos, A. Z. How Good Is Conformal Solutions Theory for Phase Equilibrium Predictions? *Fluid Phase Equilib.* **1991**, *65*, 1.
- Huang, S. H.; Radosz, M. Equation of State for Small, Large, Polydisperse, and Associating Molecules. *Ind. Eng. Chem. Res.* **1990**, *29*, 2284.
- Huang, S. H.; Radosz, M. Equation of State for Small, Large, Polydisperse, and Associating Molecules. Extension to Fluid Mixtures. *Ind. Eng. Chem. Res.* **1991**, *30*, 1994.
- Ikonomou, G. D.; Donohue, M. D. Thermodynamics of Hydrogen-Bonded Molecules: the Associated Perturbed Anisotropic Chain Theory. *AIChE J.* **1986**, *32*, 1716.
- Jackson, G.; Chapman, W. G.; Gubbins, K. E. Phase Equilibria of Associating Fluids Spherical Molecules with Multiple Bonding Sites. *Mol. Phys.* **1988**, *65*, 1.
- Johnson, J. K.; Gubbins, K. E. Phase Equilibria for Associating Lennard-Jones Fluids from Theory and Simulation. *Mol. Phys.* **1992**, *77*, 1033.
- Johnson, J. K.; Zollweg, J. A.; Gubbins, K. E. The Lennard-Jones Equation of State Revisited. *Mol. Phys.* **1993**, *78*, 591.
- Johnson, J. K.; Müller, E. A.; Gubbins, K. E. Equation of State for Lennard-Jones Chains. *J. Phys. Chem.* **1994**, *98*, 6413.
- Joslin, C. G.; Gray, C. G.; Chapman, W. G.; Gubbins, K. E. Theory and Simulation of Associating Liquid Mixtures: II. *Mol. Phys.* **1987**, *62*, 843.
- Kay, W. B. Liquid-Vapor Phase Equilibrium Relations in the Ethane-*n*-Heptane System. *Ind. Eng. Chem.* **1938**, *30*, 459.
- Kay, W. B. Liquid-Vapor Equilibrium Relations in Binary Systems. *Ind. Eng. Chem.* **1941**, *33*, 590.
- Lee, K. H.; Lombardo, M.; Sandler S. I. The Generalized van der Waals Partition Function. II. Application to the Square-Well Fluid. *Fluid Phase Equilib.* **1985**, *21*, 177.
- Matschke, D. E.; Thodos, G. Vapor-Liquid Equilibria for the Ethane-Propane System. *J. Chem. Eng. Data* **1962**, *7*, 232.
- Mehra, V. S.; Thodos, G. Liquid-Vapor Equilibria for the Ethane-*n*-Butane System. *J. Chem. Eng. Data* **1965**, *10*, 307.
- Mehra, V. S.; Thodos, G. Vapor-Liquid Equilibrium Constants for the Ethane-*n*-Butane-*n*-Heptane System at 150°, 200°, and 250 F. *J. Chem. Eng. Data* **1966**, *11*, 365.
- Müller, E. A.; Gubbins, K. E. An Equation of State for Water from a Simplified Intermolecular Potential. *Ind. Eng. Chem. Res.* **1995**, *34*, 3662.
- Müller, E. A.; Vega, L. F.; Gubbins, K. E. Theory and Simulation of Associating Fluids: Lennard-Jones Chains with Association Sites. *Mol. Phys.* **1994**, *83*, 1209.
- Müller, E. A.; Vega, L. F.; Gubbins, K. E. Molecular Simulation and Theory of Associating Chain Molecules. *Int. J. Thermophys.* **1995**, *16*, 705.
- Nezbeda, I.; Kolafa, J.; Kalyuzhnyi, V. Primitive Model of Water: II. Theoretical Results for the Structure and Thermodynamic Properties. *Mol. Phys.* **1989**, *68*, 143.
- Panagiotopoulos, A. Z. Direct Derivation of Phase Coexistence Properties of Fluids by Monte Carlo Simulation in a New Ensemble. *Mol. Phys.* **1987**, *61*, 813.
- Panagiotopoulos, A. Z. Direct Derivation of Fluid Phase Equilibria Simulation in the Gibbs Ensemble: A Review. *Mol. Simul.* **1992**, *9*, 1.
- Press, W. H.; Teulolsky, S. A.; Vetterling, W. T.; Flannery, B. P. *Numerical Recipes In Fortran*. Cambridge University Press: Cambridge, U.K., 1986.
- Smith, B. D.; Srivastava, R. *Physical Science Data: Thermodynamic Data for Pure Compounds, Part A: Hydrocarbons and Ketones*; Elsevier: New York, 1986a; Vol. 25.
- Smith, B. D.; Srivastava, R. *Physical Science Data: Thermodynamic Data for Pure Compounds, Part B: Halogenated Hydrocarbons and Alcohols*; Elsevier: New York, 1986b; Vol. 25.
- Tavares, F. W.; Chang, J.; Sandler, S. I. Equation of State for the Square-Well Chain Fluid Based on the Dimer Version of Wertheim's Perturbation Theory. *Mol. Phys.* **1995**, *86*, 1451.
- Tsang, P. C.; White, O. N.; Perigard, B. Y.; Vega, L. F.; Panagiotopoulos, A. Z. Phase Equilibria in Ternary Lennard-Jones Systems. *Fluid Phase Equilib.* **1995**, *107*, 31.
- Walsh, J. M.; Gubbins, K. E. The Liquid Structure and Thermodynamic Properties of Lennard-Jones Spheres with Associating Sites. *Mol. Phys.* **1993**, *80*, 65.
- Wertheim, M. S. Fluids with Highly Directional Attractive Forces. I. Statistical Thermodynamics. *J. Stat. Phys.* **1984a**, *35*, 19.
- Wertheim, M. S. Fluids with Highly Directional Attractive Forces. II. Thermodynamics Perturbation Theory and Integral Equations. *J. Stat. Phys.* **1984b**, *35*, 35.
- Wertheim, M. S. Fluids with Highly Directional Attractive Forces. III. Multiple Attraction Sites. *J. Stat. Phys.* **1986a**, *42*, 459.
- Wertheim, M. S. Fluids with Highly Directional Attractive Forces. IV. Equilibrium Polymerization. *J. Stat. Phys.* **1986b**, *42*, 477.
- Wertheim, M. S. Fluids of Dimerizing Hard-Spheres, and Fluid Mixtures of Hard-Spheres and Dispheres. *J. Chem. Phys.* **1986c**, *85*, 2929.
- Wertheim, M. S. Thermodynamic Perturbation Theory of Polymerization. *J. Chem. Phys.* **1987**, *87*, 7323.
- Wichterle, I.; Kobayashi, R. Vapor-Liquid Equilibrium of Methane-Ethane System at Low Temperatures and High Pressures. *J. Chem. Eng. Data* **1972a**, *17*, 9.
- Wichterle, I.; Kobayashi, R. Vapor-Liquid Equilibrium of Methane-Propane at Low Temperatures and High Pressures. *J. Chem. Eng. Data* **1972b**, *17*, 4.
- Wichterle, I.; Kobayashi, R. Vapor-Liquid Equilibrium of Methane-Ethane-Propane System at Low Temperatures and High Pressures. *J. Chem. Eng. Data* **1972c**, *17*, 13.
- Zudkevitch, D.; Joffe, J. Correlation and Prediction of Vapor-Liquid Equilibria with the Redlich-Kwong Equation of State. *AIChE J.* **1970**, *16*, 112.

Received for review June 20, 1997

Revised manuscript received September 19, 1997

Accepted October 31, 1997[®]

IE970449+